AGU ADVANCING EARTH AND SPACE SCIENCES

Geophysical Research Letters

RESEARCH LETTER
10.1029/2024GL108804

# Effects of Applied Voltage on Branching of Positive Leaders in Laboratory Long Sparks

**Changzhi Peng[1,2], Zhijun Li[3], Xuekai Pei[1,2], Xiangen Zhao[4], Gaopeng Lu[5], Feifan Liu[5], Yongping Wang[6], Baoyou Zhu[5], Yu Zheng[1,2], and Xuzhu Dong[1,2]**

[1]School of Electrical Engineering and Automation, Wuhan University, Wuhan, China, [2]State Key Laboratory of Power Grid Environmental Protection, School of Electrical Engineering and Automation, Wuhan University, Wuhan, China, [3]State Key Laboratory of Power Grid Environmental Protection, China Electric Power Research Institute, Wuhan, China, [4]Department of Building Environment and Energy Engineering, The Hong Kong Polytechnic University, Hong Kong, China, [5]School of Earth and Space Sciences, University of Science and Technology of China, Hefei, China, [6]MNR Key Laboratory for Polar Science, Polar Research Institute of China, Shanghai, China

**Key Points:**

- The positive correlation between the number of positive leader branches and applied voltage is demonstrated for the first time
- As the applied voltage increased, the strike ground points of the discharge channel became more dispersed
- The average 3-D speed of the positive leader trunk channel exhibits a slight increase with the rising applied voltage

**Correspondence to:**

X. Dong,
dongxz@whu.edu.cn

**Citation:**

Peng, C., Li, Z., Pei, X., Zhao, X., Lu, G., Liu, F., et al. (2024). Effects of applied voltage on branching of positive leaders in laboratory long sparks. *Geophysical Research Letters*, *51*, e2024GL108804. https://doi.org/10.1029/2024GL108804

Received 17 FEB 2024
Accepted 23 MAY 2024

**Author Contributions:**

**Conceptualization:** Changzhi Peng
**Data curation:** Zhijun Li, Xuekai Pei, Yu Zheng
**Formal analysis:** Xiangen Zhao, Feifan Liu, Yongping Wang
**Funding acquisition:** Xuzhu Dong
**Investigation:** Gaopeng Lu, Baoyou Zhu
**Project administration:** Xuzhu Dong
**Supervision:** Xuzhu Dong
**Writing – original draft:** Changzhi Peng
**Writing – review & editing:** Changzhi Peng, Xiangen Zhao, Gaopeng Lu, Feifan Liu



## Abstract

Positive leaders branch less frequently than negative counterpart, and the physical processes and properties of positive leader branching remain a mystery. We investigated 10 m laboratory discharges under four positive voltages using a high-speed video camera. Positive leaders differ from negative leaders by either directly splitting or connecting with floating bidirectional leaders to form branching, and the number of leader branches shows a positive correlation with the applied voltage, that is, the branched channels increased from 1 to 4 when the voltage increased by a factor of 1.5. Grounding points are positioned beneath the electrode and are more concentrated with lower voltage. During the stable progression of the leader, there is a slight increase in its development speed as the applied voltage rises. When the voltage is increased by 70%, the average breakdown time decreases by 40%. These characteristics provide insights into the branching mechanism of positive leaders.

## Plain Language Summary

The discharge mechanisms in natural and laboratory discharges are highly complex. This study aims to unravel the branching mechanism of positive leaders through laboratory experiments. A specific 10 m rod-to-plate discharge gap was designed to vary the maximum applied voltage, making it possible to examine the effects of applied voltage on the leader discharging trunk and branched channels. The statistical results indicate that as the peak voltage increases, the number of leader channels during the discharging process also increases. In natural lightning, positive leader channels generally exhibit low bifurcation rates, whereas in our study, the maximum number of discharging channels reached four with a sufficiently high applied voltage. The strike ground points of the trunk channel tend to be more dispersed when the applied voltage increases. Additionally, as the voltage rises, the average propagation speed of the leader trunk channel also increases. Our study presents the first systematic findings in this field, with crucial implications for a comprehensive understanding on the leader branching process and the development of discharge models.

## 1. Introduction

Understanding the formation of discharge branches and zigzags is a fundamental and intriguing question in both laboratory discharges and natural lightning (Mansell et al., 2002). Historically, research on leader branch characteristics has primarily focused on negative leaders (Ding et al., 2021; Hill et al., 2011; H. Huang et al., 2018; Jiang et al., 2017). However, studies on characteristics of positive leader branches are relatively scarce. Positive flash channels are typically smooth and unbranched (Nag & Rakov, 2012). As a result, the characteristics and underlying physical processes of positive leader branches remain poorly understood.

Here, we provide a concise overview of the characteristics of negative leaders. It is widely recognized that the negative leader follows a stepping mechanism (Cooray & Arevalo, 2017; Kostinskiy et al., 2018; Pu et al., 2017). Positive streamers originate from the space leader and propagate upward toward the leader tip, while negative streamers emerge from the other end of the segment and propagate in the opposite direction (Ding et al., 2021; Gallimberti et al., 2002; Qi et al., 2016). The tortuosity of the negative leader channel is believed to be a result of the random direction of each step (Scholten et al., 2021; Schonland, 1956). Jiang et al. (2017) identified two scenarios that can lead to leader branching: the first is multiple space leaders connecting to the same leader channel, and the second is space leaders/stems connecting a leader in a different direction.

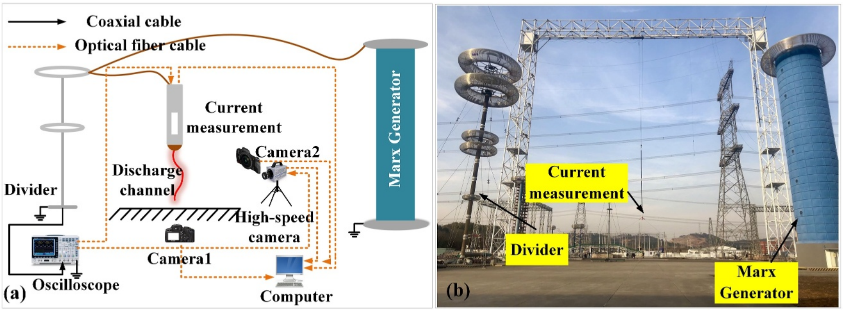


**Figure 1.** Arrangement of a 10 m rod-to-plate air gap discharge test platform. (a) Schematic diagram of test equipment arrangement, including the current measurement unit, voltage measurement unit, a high-speed video camera, and two static cameras. (b) On-site image of the outdoor test platform, with clear markings indicating the Marx generator, voltage divider, and current measurement unit.

The research on positive leader has been primarily focused on investigating fundamental physical processes, initiation meteorological conditions, velocity-current relationships, and analysis of two-dimensional (2-D) velocity (Kitagawa & Michimoto, 1994; Nag & Rakov, 2009; Saba et al., 2009; Yuan et al., 2017). Extensive studies have been conducted to explore leader stepping, cloud charge configurations, electric field (*E*-field) waveforms, multiplicity and transferred charge (Qie et al., 2005; Lu et al., 2009, 2016; Saba et al., 2010; S. Huang et al., 2022; Wang et al., 2023). Nag and Rakov (2012) reported on the investigation of cloud charge configurations, identifying at least six configurations capable of producing downward positive lightning discharges. In terms of the velocity-current relationship, the correlation between leader velocity ($v_L$) and leader current ($i_L$) is commonly described as $v_L \sim {i_L}^{\alpha}$, with $\alpha$ values varying between 0.3 and 0.67 (Andreev et al., 2008; Hutzler & Hutzler-Barre, 1982; Zhao, He, & He, 2016). Moreover, the positive leader development velocity has been observed to range from $0.23 \times 10^5$ to $17.1 \times 10^5$ m/s in different studies (Gao et al., 2014; Kong et al., 2008; Lyu et al., 2013; Saba et al., 2008). Despite these advances, reports on three-dimensional (3-D) velocity characteristics of positive leaders are limited due to the challenges and scarcity of 3-D observations. Furthermore, one notable feature in both lightning discharge and laboratory discharge, which has received relatively less attention compared to negative lightning, is the branching mechanism of positive leader.

Positive leader branching could be a cause of positive leader tip split or float bidirectional leader connection (Yuan et al., 2019). Leader branching has been observed to exhibit a relationship with discharge current and air pressure. Zhao, He, He, Li, and Huo (2016) discovered that leader current waveform spikes were associated with leader branching, indicating an increase in current during branching. Ma et al. (2019) reported that positive leaders tend to branch more easily at higher air pressure. Similarly, branching characteristics have also been studied in streamer discharges. Liu and Pasko (2004) conducted numerical simulations and found that photoionization can lead to positive streamer branching. However, in the case of positive leader, it is still unclear what factors promote leader branching and further research is needed to investigate this phenomenon.

In this study, we provide optical recordings of positive leader branches, capturing their branching and zigzagging behavior with a remarkable temporal resolution of 200,000 frames per second (fps). This high-speed recording allows for a detailed analysis on the characteristics of positive leader branches. Firstly, we investigate the properties of leader branching across different voltage levels. Furthermore, we examine the development trends of the leader channel. Finally, we present the 3-D velocity distributions of the leader trunk channel at varying voltage levels.

## 2. Experimental Instruments

The experimental data utilized in this paper were obtained from an outdoor test laboratory situated at the National Engineering Laboratory of UHV Engineering Technology in Wuhan, Hubei Province. Figure 1 illustrates the schematic diagram and test setup of the experimental equipment. This experimental platform consists of a high-voltage power supply, electrode structure, data acquisition system, and data storage system. The high-voltage power supply was a Marx generator, which could generate an impulse voltage up to 7.5 MV. The test platform included a 10 m rod-to-plate gap. The rod electrode was made of copper and with a diameter of 2 cm. The

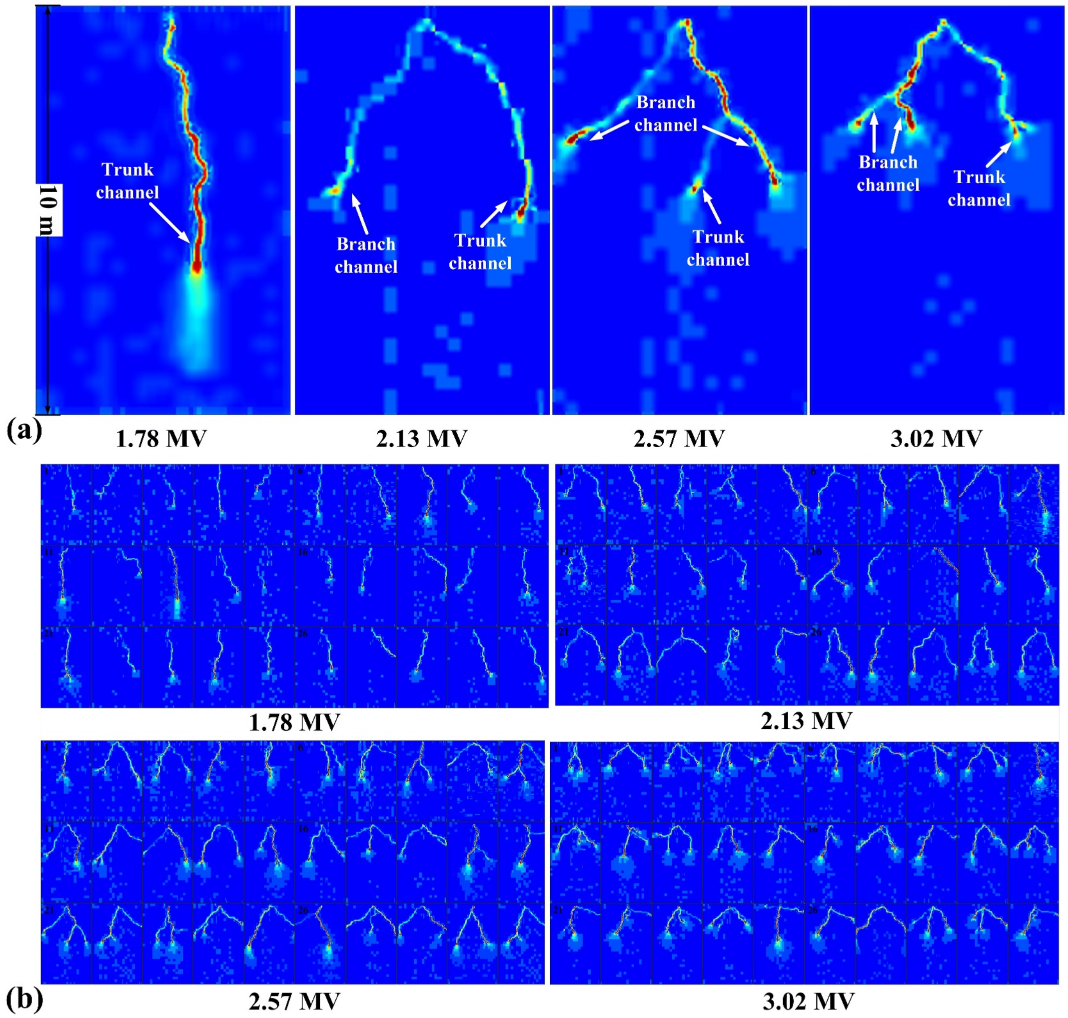


**Figure 2.** Leader channels under four different voltages. (a) Typical positive leader channels at 464, 336, 314, 271 μs (from left to right) under four different applied voltages. For 1.78, 2.13, 2.57, and 3.02 MV, the number of bright and long branched channels is 1, 2, 3, and 4, respectively. (b) Discharge channel frames during 30 discharge events under different peak voltages.

plate electrode was a well-grounded iron plate measuring $20 \times 20$ m$^2$. The high-speed video camera (Photron SA-Z CMOS) was configured with a frame rate set to 200,000 FPS, featuring a single frame resolution of $176 \times 384$ pixels. Two orthogonal constrained cameras were applied to reconstruct the 3-dimensional (3D) discharge channel. The two still cameras are Nikon D750 with an exposure time of 5 ms. A digital oscilloscope and a current sensor were employed for recording voltage and current waveform, respectively. Additional details regarding the experimental setup can be found in Peng et al. (2022).

The experiments were conducted in winter, with an absolute humidity ranging from 3 to 5 g/m³. The average dry temperature was 3.2°C, and the wet temperature was 0°C. Additionally, the air pressure in the experimental environment was at standard atmospheric pressure.

## 3. Results

### 3.1. Effect of Applied Voltage on Leader Branching

Figure 2a shows the leader development under four different patterns of applied voltage, that is, 1.78, 2.13, 2.57, and 3.02 MV. For each voltage, 30 gap breakdown tests were conducted. It can be observed that there are few bifurcations under the 1.78 MV voltage and the discharge channels appear relatively concentrated. Conversely, at

**Table 1**
*Statistics for the Number of Leader Discharge Channels During Leader Development for Discharge Breakdown Events, Under Four Different Applied Voltages*

| Applied voltage | Single channel | Two branched channels | More than two branched channels |
|---|---|---|---|
| 1.78 MV | 30 | 0 | 0 |
| 2.13 MV | 8 | 22 | 0 |
| 2.57 MV | 0 | 21 | 9 |
| 3.02 MV | 0 | 7 | 23 |

the applied voltage of 3.02 MV, three long leader branched channels are observed, with two small initial branches in the process of growth. The light intensity of the discharge channels is represented by pseudo-color, with red indicating brightness and blue representing darkness.

It is important to note that the phenomena depicted in Figure 2a are not unique. In Figure 2b, we have shown 30 images of leader channels at various voltages, providing a more comprehensive view. During each discharging process, the selected discharge trunk channel (i.e., the channel finally reaching ground) has developed to a length of 6–8 m within the 10 m air gap. The discharge lasted approximately 310, 350, 420, and 460 μs, reaching the position depicted in Figure 2a, for voltage levels of 1.78, 2.13, 2.57, and 3.02 MV, respectively. During this period, the leader trunk and branch channels (i.e., the channel eventually failing to reach grounded) reach maturity and exhibit clear luminosity, making them easily distinguishable. If the air gap experiences a complete breakdown, the light emitted from the trunk channel will overshadow that of the branch channel. As the applied voltage is increased, the leader channels become more randomized and spread out. Furthermore, an increasing number of branches emerge along the discharge channel.

At the applied voltage of 1.78 MV, no prominent bright branch channels are visible along the leader's trunk channel. However, upon careful examination of each frame of the main channel, it can be observed that there are a few minor branches near the leader's discharge channel. These minor branches can be observed in Frame 21 of Figure 2b. These small branches contribute to the zigzagging of the leader discharge channel (Zhao, He, & He, 2016). When the applied voltage is increased to 2.13 MV, it becomes easier to generate two light branches along the discharge channel. This is evident in the images captured in Figure 2b. Regardless of whether the applied voltage is 2.57 MV or 3.02 MV, the leader channel is accompanied by three or four leader branches. These branches are clearly visible in the images presented in Figure 2b.

Table 1 provides a summary of the number of evident branch channels observed during the leader discharge at various voltages. At the applied voltage of 1.78 MV, all recorded discharge events exhibited a single leader channel, representing 100% of the cases. When the applied voltage increased to 2.13 MV, the proportion of discharge events with a single leader channel decreased to 26.6%, while the proportion of events with double leader channels increased to 73.4%. At the applied voltage of 2.57 MV, 70% of the recorded discharge events displayed two clearly branched channels, while the remaining 30% exhibited three branched channels. With a higher amplitude of 3.02 MV, discharge events with two branches accounted for 23.3%, while events with three or more channels represented 76.7% of the total.

### 3.2. Effect of Applied Voltage on Leader Strike Points

To investigate the influence of applied voltages on the zigzagging of leader channels, we conducted a study by counting the locations of leader strike points on the ground. The density distribution of these strike points is presented in Figure 3a. Under the 1.78 MV applied voltage, the leader strike points appear to be more concentrated. The majority of strike points are located within a circle with a radius of 2 m below the vertical electrode, accounting for 67.5% of the total. For discharging events with applied voltages of 2.13, 2.57, and 3.02 MV, the strike ground points appear to be more dispersed. There is no significant difference in the distribution of strike ground points among these voltage levels. The average locations under each applied voltage are (0.9, 0.9) m, (−0.1, 0.2) m, (0.4, −0.3) m, and (−0.1, −0.2) m for 1.78, 2.13, 2.57, and 3.02 MV, respectively. Furthermore, Figure 3b illustrates the density distribution of strike points under the four applied voltages. It can be observed that the ground strike points are primarily clustered around the center along the $x$-axis and $y$-axis. From a two-dimensional (2D) perspective, the core strike points are located at approximately (0.9, −1.3) m. Overall, the

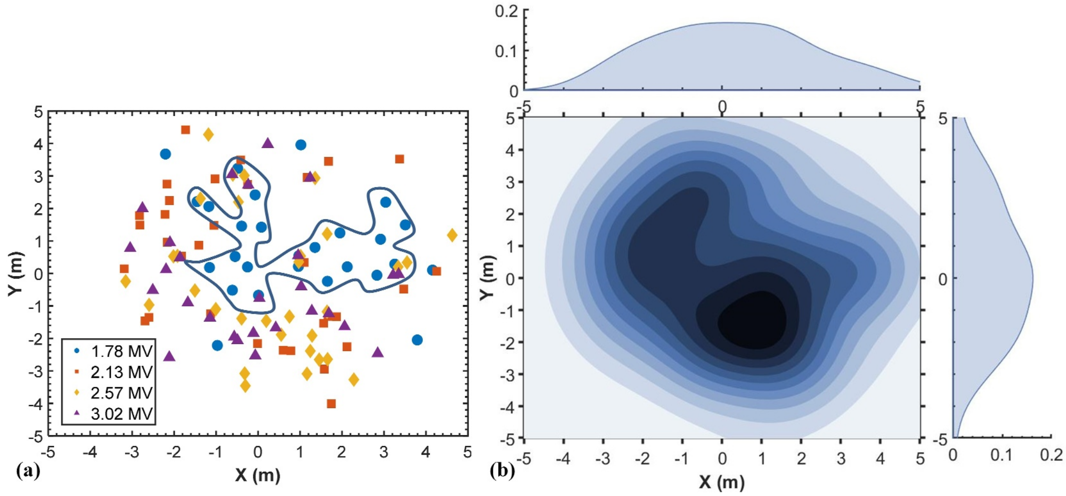


**Figure 3.** Leader strike point locations on the ground. (a) Scatter plot distribution of the leader strike location, with the portion circled by a solid line indicating the strike location at an applied voltage of 1.78 MV. (b) Density distribution of all strike points. The maximum density of the strike points is located near the center of the *x*-axis and *y*-axis, which is directly below the electrode.

results indicate that the base point of the strike is still close to the bottom of the anode, but there is some deviation in its precise location.

The standard deviations of strike locations were statistically analyzed for different branching probabilities. A larger standard deviation indicates a more dispersed impact location. For voltage levels of 1.78, 2.13, 2.57, and 3.02 MV, the corresponding standard deviation was 2.36, 3.21, 2.78, and 2.60 m, respectively. That is, among the four applied voltages used in our study, the greatest variation in the distance of impact location is reached for 2.13 MV. In the case of a single discharge channel, the standard deviation of impact location distribution was the smallest. With increasing applied voltages, the number of leader branches also increased. The increased number of branches leads to the discharge trunk channel for breakdown not being concentrated directly beneath the electrode. It is hypothesized that the channels of branching discharges bring more randomness to the propagation channel, subsequently affecting the final strike points.

### 3.3. Three-Dimensional (3-D) Velocity of Positive Trunk Leader

The positive laboratory discharge at peak voltages of 1.78, 2.13, 2.57, and 3.02 MV were comprehensively captured using our orthogonally placed single-lens cameras and a high-speed video camera. These cameras enabled us to obtain images that were used to reconstruct the 3-D path of the leader channel. The process of reconstructing a 3-D channel from two views has been extensively described by Gao et al. (2014). The upward positive leader discharge model currently mainly used 2-D data for analysis due to the limited availability of 3-D data (Becerra & Cooray, 2008). In Figure 4a, we present the reconstructed 3-D leader trunk channel and branch channel. The color of the points in the figure corresponds to the vertical height at which the leader has developed. It is important to note that the leader originates from the tip of the positive electrode, which is located 10 m above the ground. By utilizing the reconstructed 3-D path of the leader channel, we can examine the characteristics of development for both leader trunk and branched channels.

We calculate the velocity of the leader trunk channel at different crest applied voltages, including 1.78, 2.13, 2.57, and 3.02 MV. Figure 4b illustrates the vertical growth distance of the trunk leader over time, ranging from 0 to 10 m, for each voltage level. The average breakdown times for these voltages were found to be 577, 532, 440, and 390 μs, respectively. Notably, when the voltage increases by a factor of 1.7, the breakdown time decreases to approximately 0.6 times the original value. This trend suggests that as the applied voltage increases, the average development velocity of the final jump process also increases.

Figure 4c provides insights into the 3-D development velocity of the leader under different peak voltages. In the early stage of leader development, the peak voltage does not have a significant impact on the velocity. The leader

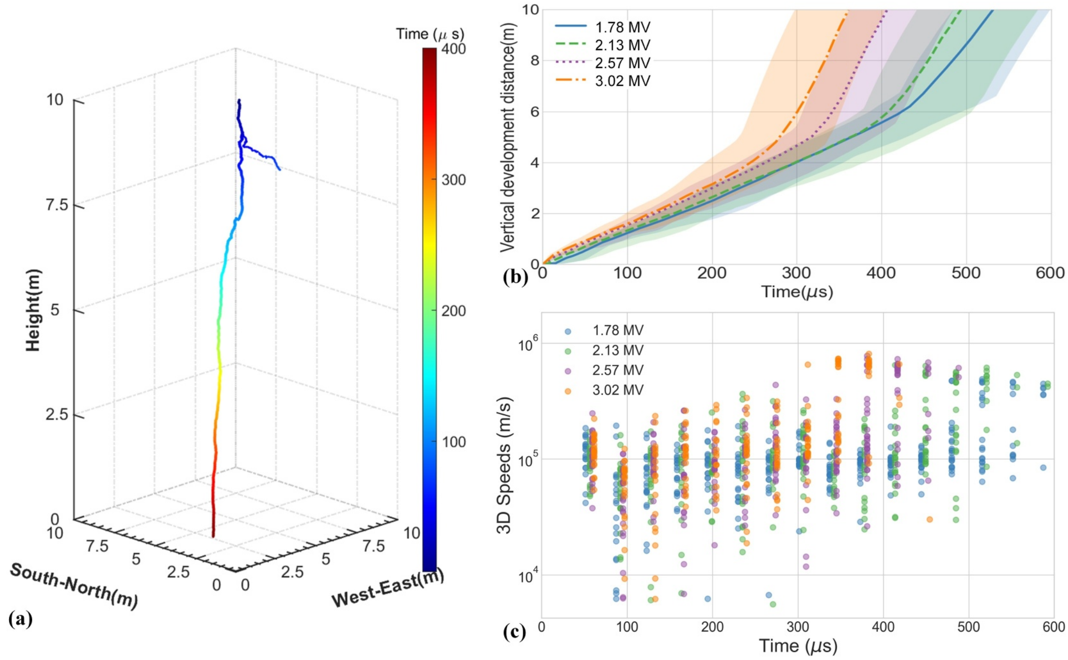


**Figure 4.** The positive leader 3-D development characteristics under different applied voltages. (a) 3-D leader discharge channel reconstruction based on orthogonal images, with applied voltage of 2.13 MV, accompanied by leader branching channel. (b) Distribution of vertical development distance of leaders over time under four different peak voltages (1.78, 2.13, 2.57, and 3.02 MV). (c) Distribution of 3-D development speed of leaders over time under four different peak voltages (1.78, 2.13, 2.57, and 3.02 MV).

usually extends at a 3-D velocity below $10^5$ m/s during this stage. However, as the leader continues to develop and enters into the final jump stage, closer to the ground, the voltage level becomes more influential. From Figures 4b and 4c, it is evident that as the applied voltage increases, the time to reach the final jump stage occurs earlier, and the height of the final jump is higher. Specifically, at the applied voltage of 3.02 MV, the maximum 3-D development speed during the final jump stage can reach $6 \times 10^5$ m/s. Which is to say, as the applied voltage decreases, the development velocity during the grounding process gradually decreases as well. The average 3-D speeds for the entire discharge process are $3.28 \times 10^4$ m/s, $3.53 \times 10^4$ m/s, $3.89 \times 10^4$ m/s, and $4.33 \times 10^4$ m/s for 1.78, 2.13, 2.57, and 3.02 MV, respectively. The entire discharge process means that the leader's vertical development distance ranges from 0 to 10 m, as shown in Figure 4b. Due to the limitations of the statistical process, not all leader branches could be reconstructed in 3-D. The average 2-D speeds the branches were measured to be $1.05 \times 10^4$ m/s, $1.44 \times 10^4$ m/s, and $1.95 \times 10^4$ m/s for voltages of 2.13, 2.57, and 3.02 MV, respectively.

## 4. Discussions

The formation of positive leader branches is a fundamental issue in lightning physics and studies on laboratory air gap discharge. We made an intriguing discovery in this study that the application of voltage visibly promotes the formation of leader branching. When the voltage is applied at approximately 50% of the breakdown voltage, there are minimal branched channels formed along the leader discharge trunk channel. However, when the voltage is increased by 1.5 times, the leader discharge channel becomes accompanied by two distinct and long branching channels. Coleman et al. (2003) found a strong correlation between lightning branched channels and electric potential extrema, suggesting a necessary condition for leader branching. Similarly, Lalande and Mazur (2012) interpreted the branching of upward positive leaders from tall towers as a result of high *E*-field changes, indicating significant potential drop values. The results observed in our study are consistent with these explanations. Furthermore, Figure 2b illustrates that most of the leader branches initiate at the electrode head. This observation can be attributed to the fact that the *E*-field at the electrode head is directly influenced by the applied voltage. We speculate that the increase in applied voltage results in an enhanced *E*-field at both the electrode head and the leader tip, thereby intensifying local ionization activity. This enhanced ionization activity leads to instability in

10.1029/2024GL108804

the distribution of local electrons, consequently promoting the formation of branches in the leader. In addition to the branching phenomena observed in positive leader discharge, similar branching can also occur in the streamer discharge at the head of the leader. Liu and Pasko (2004) used a physical model to investigate the formation of streamer discharge branching. They found that photoionization plays a critical role in streamer branching process. Furthermore, the formation of streamer discharge branching may also contribute to the generation of leader branching.

In our study, the 3-D speed of the positive leader ranges from $0.01 \times 10^5$ to $6.01 \times 10^5$ m/s. This speed is influenced by the ambient *E*-field, which correlates with the height of the leader tip above the ground and increases as the propagation advances. Laboratory-scale discharges conducted by the Les Renardières Group (1977) obtained 2-D speeds ranging from $0.12 \times 10^5$ to $0.42 \times 10^5$ m/s. The average 2-D leader velocity varies from $0.08 \times 10^5$ to $0.15 \times 10^5$ m/s under a 3-m air gap discharge (Gu et al., 2010). Saba et al. (2008) reported 2-D speeds for nine natural positive cloud-to-ground leaders, ranging from $0.23 \times 10^5$ to $13.0 \times 10^5$ m/s. For natural upward positive leaders, the 3-D speed values range from $0.8 \times 10^5$ m/s to $14.3 \times 10^5$ m/s (Gao et al., 2014). The 2-D speed of triggered upward positive leaders increases with altitude, ranging from $0.55 \times 10^5$ to $2.1 \times 10^5$ m/s (Biagi et al., 2011).

The 3-D velocities of positive leader observed in both negative cloud-to-ground and intra-cloud flashes are in the range of $1–3 \times 10^4$ m/s (Wu et al., 2019). The 3-D velocities of positive leader in positive cloud-to-ground exhibit significant variability, spanning orders of magnitude from $10^4$ to $10^6$ m/s. Wu et al. (2019) noted that the horizontal development speed of positive leader within thundercloud is relatively slow ($\sim 10^4$ m/s) and stable, likely due to the relatively stable *E*-field inside cloud.

Figures 4b and 4c illustrate that there is minimal disparity in the development speed of the leader trunk channel during the initial 5 m of growth. At this initial phase, the trunk channel tends to expand alongside branched channels as the electric field intensifies. This phenomenon suggests that the development of branching channels might draw some energy from the trunk channel, consequently impeding a substantial acceleration in the growth rate of the trunk channel. As discussed by Zhao et al. (2019), the discharge current of the leader needs to be distributed among the branches to establish a relationship between the discharge current and the leader's development velocity.

The observed leader branching mode and development velocities in this study are of significant reference value for constructing physical models of positive polarity long air gap discharge and relevant lightning models. It is evident that the *E*-field at the head of the positive leader plays a crucial role in the branching of the positive leader (Lalande & Mazur, 2012). In the later stages, the influence of applied voltage on the conditions and number of leader branches can be further explored in conjunction with physical models.

## 5. Conclusions

In this study, we conducted 10 m positive long air gap discharges at different applied voltages with maximum ranging from 1.78 to 3.02 MV. By utilizing a high-speed optical observation system, we were able to characterize the positive trunk channel and branch channel of the discharges. One notable finding of this study is the positive correlation observed between the number of leader branches and the gap potential. This discovery holds significant importance in comprehending the mechanism behind positive leader branching and in constructing corresponding models for positive leader branches. Furthermore, our observations revealed that although there is a certain level of randomness in the main channel of the leader discharge, the final strike position of the channel breakdown consistently occurs very close to the bottom of the electrode. When comparing the 3-D development velocities of the leader under different applied voltages, it is observed that in the initial few meters of leader development, the speed difference in the main channel is minimal.

## Data Availability Statement

The high-speed video of positive leader observations and the associated long exposure image data used to produce the main results in this paper are publicly available at Peng et al. (2024).

**Acknowledgments**

The research is supported by National Natural Science Foundation of China - State Grid Corporation Joint Fund for Smart Grid (No: U2066217) and China Southern Power Grid Project (No: 1500002023030103GY00256). The authors would like to thank Olaf Scholten and Brian Hare from the University of Groningen for their helpful comments on this work.

## References

Andreev, A. G., Bazelyan, E. M., Bulatov, M. U., Kuzhekin, I. P., Makalsky, L. M., Sukharevskij, D. I., & Syssoev, V. S. (2008). Experimental study of the positive leader velocity as a function of the current in the initial and final-jump phases of a spark discharge. *Plasma Physics Reports*, *34*(7), 609–615. https://doi.org/10.1134/S1063780X0807009X

Becerra, M., & Cooray, V. (2008). On the velocity of positive connecting leaders associated with negative downward lightning leaders. *Geophysical Research Letters*, *35*(2), L02801. https://doi.org/10.1029/2007GL032506

Biagi, C. J., Uman, M. A., Hill, J. D., & Jordan, D. M. (2011). Observations of the initial, upward-propagating, positive leader steps in a rocket-and-wire triggered lightning discharge. *Geophysical Research Letters*, *38*(24). https://doi.org/10.1029/2011GL049944

Coleman, L. M., Marshall, T. C., Stolzenburg, M., Hamlin, T., Krehbiel, P. R., Rison, W., & Thomas, R. J. (2003). Effects of charge and electrostatic potential on lightning propagation. *Journal of Geophysical Research*, *108*(D9). https://doi.org/10.1029/2002jd002718

Cooray, V., & Arevalo, L. (2017). Modeling the stepping process of negative lightning stepped leaders. *Atmosphere*, *8*(12), 245. https://doi.org/10.3390/atmos8120245

Ding, Z., Rakov, V. A., Zhu, Y., Tran, M. D., Kostinskiy, A. Y., & Kereszy, I. (2021). Evidence and inferred mechanism of collisions of downward stepped-leader branches in negative lightning. *Geophysical Research Letters*, *48*(11). https://doi.org/10.1029/2021gl093295

Gallimberti, I., Bacchiega, G., Bondiou-Clergerie, A., & Lalande, P. (2002). Fundamental processes in long air gap discharges. *Comptes Rendus Physique*, *3*(10), 1335–1359. https://doi.org/10.1016/S1631-0705(02)01414-7

Gao, Y., Lu, W., Ma, Y., Chen, L., Zhang, Y., Yan, X., & Zhang, Y. (2014). Three-dimensional propagation characteristics of the upward connecting leaders in six negative tall-object flashes in Guangzhou. *Atmospheric Research*, *149*, 193–203. https://doi.org/10.1016/j.atmosres.2014.06.008

Gu, S., Chen, W., Chen, J., He, H., & Qian, G. (2010). Observation of the streamer–leader propagation processes of long air-gap positive discharges. *IEEE Transactions on Plasma Science*, *38*(2), 214–217. https://doi.org/10.1109/TPS.2009.2037004

Hill, J. D., Uman, M. A., & Jordan, D. M. (2011). High-speed video observations of a lightning stepped leader. *Journal of Geophysical Research*, *116*(D16), D16117. https://doi.org/10.1029/2011JD015818

Huang, H., Wang, D., Wu, T., & Takagi, N. (2018). Formation features of steps and branches of an upward negative leader. *Journal of Geophysical Research: Atmospheres*, *123*(22), 12597–12605. https://doi.org/10.1029/2018jd028979

Huang, S., Chen, W., Fu, Z., Fu, Y., Xiang, N., Qiu, X., et al. (2022). Separate luminous structures leading positive leader steps. *Nature Communications*, *13*(1), 3655. https://doi.org/10.1038/s41467-022-31409-x

Hutzler, B., & Hutzler-Barre, D. (1978). Leader propagation model for predetermination of switching surge flashover voltage of large air gaps. *IEEE Transactions on Power Apparatus and Systems*, *PAS-97*(4), 1087–1096. https://doi.org/10.1109/TPAS.1978.354588

Jiang, R., Qie, X., Zhang, H., Liu, M., Sun, Z., Lu, G., et al. (2017). Channel branching and zigzagging in negative cloud-to-ground lightning. *Scientific Reports*, *7*(1), 3457. https://doi.org/10.1038/s41598-017-03686-w

Kitagawa, N., & Michimoto, K. (1994). Meteorological and electrical aspects of winter thunderclouds. *Journal of Geophysical Research*, *99*(10), 10713–10721. https://doi.org/10.1029/94JD00288

Kong, X., Qie, X., & Zhao, Y. (2008). Characteristics of downward leader in a positive cloud-to-ground lightning flash observed by high-speed video camera and electric field changes. *Geophysical Research Letters*, *35*(5). https://doi.org/10.1029/2007GL032764

Kostinskiy, A. Y., Syssoev, V. S., Bogatov, N. A., Mareev, E. A., Andreev, M. G., Bulatov, M. U., et al. (2018). Abrupt elongation (stepping) of negative and positive leaders culminating in an intense corona streamer burst: Observations in long sparks and implications for lightning. *Journal of Geophysical Research: Atmospheres*, *123*(10), 5360–5375. https://doi.org/10.1029/2017jd027997

Lalande, P., & Mazur, V. (2012). In *A physical model of branching in upward leaders* (Vol. 5, pp. 1–7). Aerospace Lab. Retrieved from https://hal.science/hal-01184412

Les Renardières Group. (1977). Positive discharges in long air gaps at Les Renardières, 1975 results and conclusions. *Electra*, *53*, 31–153.

Liu, N., & Pasko, V. P. (2004). Effects of photoionization on propagation and branching of positive and negative streamers in sprites. *Journal of Geophysical Research*, *109*(A4). https://doi.org/10.1029/2003JA010064

Lu, G., Cummer, S. A., Li, J., Han, F., Blakeslee, R. J., & Christian, H. J. (2009). Charge transfer and in-cloud structure of large-charge-moment positive lightning strokes in a mesoscale convective system. *Geophysical Research Letters*, *36*(15). https://doi.org/10.1029/2009GL038880

Lu, G., Zhang, H., Jiang, R., Fan, Y., Qie, X., Liu, M., et al. (2016). Characterization of initial current pulses in negative rocket-triggered lightning with sensitive magnetic sensor. *Radio Science*, *51*(9), 1432–1444. https://doi.org/10.1002/2016rs005945

Lyu, W., Chen, L., Ma, Y., Rakov, V. A., & Gao, Y. (2013). Lightning attachment process involving connection of the downward negative leader to the lateral surface of the upward connecting leader. *Geophysical Research Letters*. https://doi.org/10.1002/2013GL058060

Ma, X., Zhuang, C., Wang, Z., & Zeng, R. (2019). Positive leader velocity and discharge current considering leader branching under different air pressures. *IEEE Transactions on Plasma Science*, *47*(5), 1939–1943. https://doi.org/10.1109/TPS.2018.2886570

Mansell, E. R., MacGorman, D. R., Ziegler, C. L., & Straka, J. M. (2002). Simulated three-dimensional branched lightning in a numerical thunderstorm model. *Journal of Geophysical Research*, *107*(D9), ACL2-1–ACL2-12. https://doi.org/10.1029/2000jd000244

Nag, A., & Rakov, V. A. (2009). Some inferences on the role of lower positive charge region in facilitating different types of lightning. *Geophysical Research Letters*, *36*(5), L05815. https://doi.org/10.1029/2008GL036783

Nag, A., & Rakov, V. A. (2012). Positive lightning: An overview, new observations, and inferences. *Journal of Geophysical Research*, *117*(D8). https://doi.org/10.1029/2012jd017545

Peng, C., Dong, X., Zhao, Y., Li, Z., Zheng, Y., Pei, X., et al. (2022). Discharge characteristics of leader inception and development under 10-meter long air gap—Experimental observation and simulation results. *High Voltage*, *8*(6), 1151–1160. https://doi.org/10.1049/hve2.12288

Peng, C., Li, Z., & Dong, X. (2024). High-speed video observations on positive leader branching under different applied voltages (Version 1.0) [Dataset]. *Zenodo*. https://doi.org/10.5281/zenodo.10673325

Pu, Y., Jiang, R., Qie, X., Liu, M., Zhang, H., Fan, Y., & Wu, X. (2017). Upward negative leaders in positive triggered lightning: Stepping and branching in the initial stage. *Geophysical Research Letters*, *44*(13), 7029–7035. https://doi.org/10.1002/2017GL074228

Qi, Q., Lu, W., Ma, Y., Chen, L., Zhang, Y., & Rakov, V. A. (2016). High-speed video observations of the fine structure of a natural negative stepped leader at close distance. *Atmospheric Research*, *178–179*, 260–267. https://doi.org/10.1016/j.atmosres.2016.03.027

Qie, X., Zhang, T., Chen, C., Zhang, G., Zhang, T., & Wei, W. (2005). The lower positive charge center and its effect on lightning discharges on the Tibetan Plateau. *Geophysical Research Letters*, *32*(5), L05814. https://doi.org/10.1029/2004GL022162

Saba, M. M. F., Campos, L. Z. S., Krider, E. P., & Pinto, O., Jr. (2009). High-speed video observations of positive ground flashes produced by intracloud lightning. *Geophysical Research Letters*, *36*(12), L12811. https://doi.org/10.1029/2009GL038791

Saba, M. M. F., Cummins, K. L., Warner, T. A., Krider, E. P., Campos, L. Z. S., Ballarotti, M. G., et al. (2008). Positive leader characteristics from high-speed video observations. *Geophysical Research Letters*, *35*(7). https://doi.org/10.1029/2007GL033000

Saba, M. M. F., Schulz, W., Warner, T. A., Campos, L. Z. S., Schumann, C., Krider, E. P., et al. (2010). High-speed video observations of positive lightning flashes to ground. *Journal of Geophysical Research*, *115*(D24). https://doi.org/10.1029/2010JD014330

Scholten, O., Hare, B. M., Dwyer, J., Liu, N., Sterpka, C., Buitink, S., et al. (2021). Time resolved 3D interferometric imaging of a section of a negative leader with LOFAR. *Physical Review D*, *104*(6), 063022. https://doi.org/10.1103/PhysRevD.104.063022

Schonland, B. F. J. (1956). In *The lightning discharge, Encyclopaedia of Physics* (Vol. 22, pp. 576–628). Springer-Verlag.

Wang, Z., Lu, G., Li, X., Zhang, H., Fan, Y., Ren, H., et al. (2023). Low frequency magnetic field observations of natural positive leaders featuring stepwise propagation. *Geophysical Research Letters*, *50*(20). https://doi.org/10.1029/2023gl105540

Wu, T., Wang, D., & Takagi, N. (2019). Velocities of positive leaders in intracloud and negative cloud-to-ground lightning flashes. *Journal of Geophysical Research: Atmospheres*, *124*(17–18), 9983–9995. https://doi.org/10.1029/2019JD030783

Yuan, S., Jiang, R., Qie, X., Sun, Z., Wang, D., & Srivastava, A. (2019). Development of side bidirectional leader and its effect on channel branching of the progressing positive leader of lightning. *Geophysical Research Letters*, *46*(3), 1746–1753. https://doi.org/10.1029/2018gl080718

Yuan, S., Jiang, R., Qie, X., Wang, D., Sun, Z., & Liu, M. (2017). Characteristics of upward lightning on the Beijing 325 m meteorology tower and corresponding thunderstorm conditions. *Journal of Geophysical Research: Atmospheres*, *122*(22), 12093–12105. https://doi.org/10.1002/2017JD027198

Zhao, X., He, J., & He, H. (2016). Effect of branching on spikes of positive leader current. *IEEE Transactions on Dielectrics and Electrical Insulation*, *23*(4), 1–6. https://doi.org/10.1109/TDEI.2016.7556468

Zhao, X., He, J., He, H., Li, Z., & Huo, F. (2016b). Effect of branching on the channel tortuosity of positive leader. *IEEE Transactions on Dielectrics and Electrical Insulation*, *23*(5), 2501–2504. https://doi.org/10.1109/TDEI.2016.7736805

Zhao, X., Liu, L., Yue, Y., He, H., Liu, L., & He, J. (2019). On the use of quantitative Schlieren techniques in temperature measurement of leader discharge channels. *Plasma Sources Science and Technology*, *28*(7), 075012. https://doi.org/10.1088/1361-6595/ab1c3e